DC Plasma-Polymerization of Pyrrole: Comparison of Films Formed on Anode and Cathode

S. EUFINGER,[1] W. J. VAN OOIJ,[2,*] and T. H. RIDGWAY[1]

[1]Department of Chemistry and [2]Department of Material Science and Engineering, University of Cincinnati, Cincinnati, Ohio 45221

SYNOPSIS

Thin films of plasma-polymerized pyrrole were deposited on stainless steel substrates from a parallel-plate DC reactor. They were characterized by XPS, ^{1}H-NMR, STM, cyclic voltammetry, and by reflection–absorption infrared (RAIR) and UV-VIS spectroscopy. The films simultaneously formed on the anode and the cathode were compared. Substantial differences were found between the structures of these films, although their overall compositions were very similar. The films on the anode appeared to be less crosslinked and contained less unsaturation and conjugation than the films on the cathode. The observed effects are explained in a model in which the concurrent positive ion bombardment plays an important role in modifying the structure of a growing plasma-polymerized film. © 1996 John Wiley & Sons, Inc.

INTRODUCTION

The preparation and investigation of conductive polymer films has been a very active field of research for nearly two decades. Polypyrrole was among the first electroresponsive polymers studied.[1] The films have been found to be conductive upon oxidation, the conductivity depending largely on the type of anion used for doping.[2] These polymers have been extensively characterized by various electrochemical and spectroscopic methods.[3] As opposed to the wealth of information published on electrochemically polymerized pyrrole, there are very few reports on plasma polymerization of this monomer.[4,5]

Plasma polymerization of organic monomers has received a considerable amount of interest over the last few years. It has several potential advantages over the electrochemical or chemical preparation of polymer films. These include: low permeability for oxygen, water vapor, and various ions; good adhesion to substrates or topcoats; high resistance to commonly used solvents; and the ability to alter certain properties of the film by changing plasma parameters.[6] An additional benefit of the polymerization process is that it is solvent-free and requires little energy, thus making it environmentally friendly. Plasma-deposited films have been used mostly as protective coatings,[7] but their potential field of application is much broader.[8]

Most plasma polymerization to date has been performed with glow discharges created by AC (50 Hz–5 kHz), RF (13.56 MHz), or a microwave (2.45 GHz).[6] Polymerization by a DC glow discharge has not been popular because of several perceived disadvantages, such as the requirement of a conductive substrate and the inhibition of film growth due to the buildup of a nonconductive coating.[6] Recent work has demonstrated that these problems can be resolved and pinhole-free films with good adhesion to the substrate can be obtained.[7,9,10]

In previous publications it was shown that the pyrrole ring is not preserved in the DC plasma and so the structure of the films does not resemble that of electrochemically polymerized pyrrole. It was found that the monomer pressure during the deposition had the strongest influence on the film structure. High pressure led to a dense, more hydrogenated film, while low pressure resulted in a loosely

* To whom all correspondence should be addressed.

Journal of Applied Polymer Science, Vol. 61, 1503–1514 (1996)
 CCC 0021-8995/96/091503-12

packed, more carbon-like film with considerably less hydrogen.[11] It was also found that the amount of ion bombardment during deposition had a marked influence on the film structure.[12]

In the study reported here, we have investigated the possible influence of positive and negative ions on the film structure of plasma-polymerized pyrrole by comparing the composition and structure of films simultaneously deposited on the cathode and anode of a parallel-plate DC plasma reactor. Although deposition in such a reactor occurs predominantly on the cathode, some deposition takes place on the anode as well.[11,12] The analytical techniques used are reflection-absorption infrared spectroscopy (RAIR), X-ray photoelectron spectroscopy (XPS), scanning tunneling microscopy (STM), ultraviolet-visible spectroscopy (UV-VIS), nuclear magnetic resonance (NMR), and cyclic voltammetry (CV).

EXPERIMENTAL

Materials

The substrate materials used were 434 bright-annealed stainless steel (Armco Inc., Middletown, OH), quartz cuvettes (Fisher Scientific; Fair Lawn, NJ), Pt disk electrodes (Bioanalytical Systems; West Lafayette, IN), and highly polished Pt foil (Denton Vacuum Inc.; Cherry Hill, NJ). The pyrrole had a purity of 98% (Aldrich Chemical Company Inc.; Milwaukee, WI) and was used as received.

Potassium bromide with a purity of 99%+ (Aldrich Chemical Company Inc.; Milwaukee, WI), potassium ferricyanide (99%+) (Aldrich Chemical Company Inc.; Milwaukee, WI), tetraethylammonium fluoroborate (99%+) (Southwestern Analytical Chemicals Inc.; Austin, TX) and acetonitrile (99.9%) (Fisher Scientific; Fair Lawn, NJ) were used as received in the cyclic voltammetry experiments.

The d_6-acetone used in the NMR experiment had a purity of 99.8% (Fluka; Ronkonkoma, NY). The acetone used for cleaning of the samples had a purity of 99.7% (Fisher Scientific; Fair Lawn, NJ) and was dried over molecular sieve #3A (Aldrich Chemical Company Inc.; Milwaukee, WI). The argon gas used in the *in situ* cleaning process was of the highest available research quality (99.999%) (Wright Brothers Inc.; Cincinnati, OH).

DC-Plasma Polymerization

Plasma polymerization of pyrrole was performed in a custom-built DC plasma reactor which has been described elsewhere.[10,13] The substrates were attached to either the cathode or the anode and the deposition of the film on both substrates was performed simultaneously. These experiments were reproduced several times. Prior to introduction into the chamber, the stainless steel substrates were cleaned in an ultrasonic acetone bath for 20 min. The Pt disk electrodes were polished to a 0.03 μm mirror-polish and also cleaned in an ultrasonic acetone bath for 20 min.

After introduction of the substrate into the reactor, the chamber was evacuated to less than 10^2 Pa. It was flushed several times with argon. Further cleaning took place *in situ* by exposing the sample to an argon plasma for 25 min. The power used was 25 W, the flow rate was 5.2 sccm (standard cubic centimeters) and the pressure 16 Pa. The chamber was then pumped down again to 10^{-2} Pa and the monomer was introduced at steady flow conditions.

The plasma polymerization of pyrrole was performed for 20 min at a power of 15 W. The monomer pressure inside the reactor was 40 Pa and the flow rate was kept constant at 4.3 sccm throughout the deposition. After the reactor run, the chamber was pumped down to 10^{-2} Pa and then slowly brought up to atmospheric pressure with argon. The IR, the UV-VIS, and the XPS spectra were taken immediately after opening of the reactor. The film thickness obtained on the anode and cathode was of the order of 50 and 500 nm, respectively.

NMR

Prior to the NMR analysis the anode film was dissolved in d_6-acetone. The spectrum was recorded immediately after dissolving the film. Since the cathode film did not dissolve in any solvent, a spectrum of only the anode film is presented. ^{1}H-NMR spectra of the anode film were obtained on a Bruker 250 MHz Spectrometer at room temperature. They were averaged over 16 scans. The peak values are reported with respect to the d_6-acetone peak at 2.04 ppm. A ^{13}C-NMR spectrum could not be obtained because of the low concentration of the solution.

Infrared Spectroscopy

RAIR spectra were acquired on a BIO-RAD FTS-40 FTIR spectrometer with a BIO-RAD variable angular specular reflectance attachment, which was set to an incidence angle of 80°. The spectra were obtained using a resolution of 4 cm^{-1} and were averaged over 128 scans. A background spectrum ob-

tained with an uncoated stainless steel substrate was subtracted from the acquired spectra in all cases.

X-Ray Photoelectron Spectroscopy

XPS was performed on a Perkin Elmer model 5300 XPS spectrometer equipped with a Mg/Zr dual anode. The spectra reported here were recorded with the MgK_{α} anode operated at 300 W. The survey spectra were obtained with a pass energy of 89 eV and the narrow scans were acquired at 36 eV and 0.05 eV step size. The energy resolution of the narrow scans was 0.7 eV. An Apollo computer system with proprietary Perkin Elmer software was used for data analysis. Deconvolution was done using Gaussian peak shapes with Lorentzian tails and a Shirley background. XPS spectra were recorded with at 75° and 15° take-off angle with respect to the sample surface. Both types of films were analyzed by XPS within 30 min after deposition, thus minimizing the exposure to the atmosphere.

Scanning Tunneling Microscopy

Scanning tunneling images of both polymer films were obtained on a Burleigh Instructional Scanning Tunneling Microscope. The samples were cut to a smaller size of 1×0.5 cm^2 and mounted on a SEM sample holder using silver paint. They were then coated with a very thin (*ca.* 50 Å) layer of gold. For each image 256×256 data points were taken. The bias voltage was set at -50 mV and the tunneling current at -2 nA.

UV-VIS Spectroscopy

UV-VIS spectra of the film were recorded on a Hewlett-Packard HP 8452A diode array spectrometer. The film was deposited on a quartz cuvette on which a very thin (ca. 100 Å) layer of gold was sputtered, using a Denton Desk II cold sputter unit (Denton Vacuum, Inc., Cherry Hill, NJ). The film was thin enough to allow the transmission of UV and visible light. During the polymerization process these conductive films were then electrically and mechanically connected to cathode and anode. In every case, a background of the cuvette with the gold film was collected prior to deposition and the appropriate subtraction was performed.

Cyclic Voltammetry

The cyclic voltammograms were recorded with a BAS 100 potentiostat (Bioanalytical Systems; West Lafayette, IN). The experiments were all carried out at room temperature and at a pH of 6. The platinum disk electrode was characterized with 10 m*M* potassium ferricyanide/0.2*M* potassium chloride solution prior to coating.

In the following discussion the plasma-polymerized pyrrole film is referred to as PPy.

RESULTS

The FTIR spectra of the PPy films deposited on stainless steel as the cathode or anode, respectively, are shown in Figure 1(a) and (b). Comparison to FTIR spectra of undoped electrochemically polymerized polypyrrole-films shows little resemblance to any of the two presented spectra.[14]

Both spectra exhibit a broad band between 3300 cm^{-1} and 3400 cm^{-1}, which is due to the N—H stretching vibration of primary and secondary amines and imines. In the film deposited on the cathode [Fig. 1(a)] the relative intensity of this peak is lower than that in the anode film. Since the XPS spectra of both films show almost the same nitrogen content for both films, it is conceivable that the nitrogen in the cathode film is present primarily in the form of secondary amines or imines, which have weaker N—H absorption bands.[15]

In both spectra several intense bands slightly below 3000 cm^{-1} can be observed. They are attributed to the symmetric and asymmetric C—H stretching vibration of saturated hydrocarbons. The PPy film deposited on the anode [Fig. 1(b)] shows three clearly distinguished peaks around 2960 cm^{-1}, 2930 cm^{-1}, and 2870 cm^{-1}, with the 2960 cm^{-1} and the 2930 cm^{-1} peaks having almost the same intensity. In the cathode film [Fig. 1(a)], however, the peak at 2960 cm^{-1} is much less pronounced. Since the peak at 2930 cm^{-1} can be attributed to the asymmetric CH_2 vibration, while the band at 2960 cm^{-1} represents the asymmetric CH_3 stretch, it can be concluded that the cathode film contains more methylene groups than the anode film.

This is also corroborated by the alkane C—H deformation region around 1450 cm^{-1}. In the case of the PPy-film on stainless steel as the cathode there seems to be only one peak at 1450 cm^{-1}, which is interpreted as the —CH_2— scissor vibration. In addition to this peak, the anode spectrum exhibits bands at 1420 cm^{-1} and 1380 cm^{-1} which are due to the C—H deformation of a CH_3 group. This again shows that the cathode film on stainless steel contains more methylene groups than the anode film.

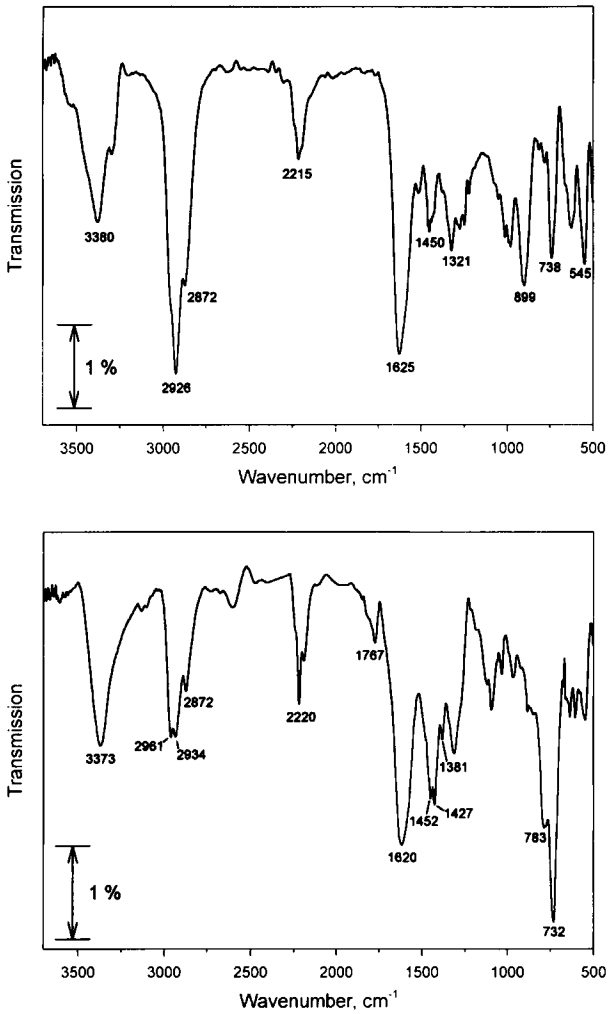

Figure 1 (a) RAIR spectrum of a PPy film deposited on stainless steel substrate as cathode; conditions: power, 15 W; pressure, 40 Pa; deposition time, 20 min; monomer flow rate, 4.3 sccm; for band assignments see text. (b) RAIR spectrum of a PPy-film deposited on stainless steel substrate as anode; conditions as in Figure 1(a); for band assignments see text.

This is further supported by the band at 1320 cm^{-1} which is interpreted as a $-C-H$ deformation vibration. This interpretation is further justified by the absorption at 545 cm^{-1} which could be caused by branched chain alkanes.[15] Both vibrations are more pronounced in the spectrum of the cathode film.

Both spectra show a band around 2220 cm^{-1} which is assigned to the $-C\equiv N$ stretching vibration. The presence of nitrile groups has also been corroborated by negative TOF-SIMS spectra.[11] The absorption seems to be more intense in case of the anode film in Figure 1(b). Figure 1(b) also displays a peak at 1767 cm^{-1}, interpreted as the $\rangle C=O$ stretching vibration, which could be caused by an amide group. This interpretation is also supported by a weak band around 3100 cm^{-1}, which can be explained as the amide $N-H$ stretch.

Common to both spectra is a strong peak around 1620 cm^{-1}, which appears to have a higher intensity in the case of the cathode films in Figure 1(a). This peak is a combination of the $C=C$ and the $C=N$ stretch and also of the $N-H$ deformation vibration. Its higher intensity in the cathode films could be due to conjugational effects.[15] In addition to that, Figure 1(a) also shows a fairly strong, broad band at 900 cm^{-1}, which is interpreted as the $C=C-H$ deformation vibration of a vinylidene group. This vibration is not found in the anode film.

The two spectra exhibit an absorption around 730 cm^{-1}, which is more intense in Figure 1(b). This absorption can be contributed to the $-CH_2-$ rocking vibration of long aliphatic chains as seen in polyethylene.[16] In the cathode case this vibration is weak, while in the anode case it is much more intense.

The IR spectra suggest substantial differences in the film structures. The cathode film seems to exhibit a higher degree of crosslinking with more unsaturation. The anode film shows a less dense structure that seems to consist to some extent of long hydrocarbon chains.

The XPS spectra for the two types of samples were very similar. The only elements that were detected were carbon, nitrogen, and small amounts of oxygen. The oxygen intensity was somewhat higher for the cathode film than for the film on the anode. For both types of films the oxygen intensity was lower at 75° take-off angle than at 15°, indicating that oxygen had probably been absorbed by the films during the short exposure to the atmosphere between deposition and analysis. The C/N ratio in both materials was approximately 6–7, i.e., higher than for the monomer (4.0). For both materials and for both take-off angles, the C1s line could be deconvoluted into a singlet at 284.6 eV and one at 286.1 eV. Since the ratio of the areas of these singlets was approximately 7/1, they must represent carbon in an approximately neutral state and carbon bonded to nitrogen. Only in the case of the cathode film at 15° take-off angle was there a third singlet peak with a 3.0 eV upward shift. This peak was most likely due to $\rangle C=O$ groups formed by adsorbed oxygen. All

singlet peaks were rather broad (2.0 eV) indicating a range of closely related structures rather than one well-defined chemical state. Such an effect can be expected for plasma-polymerized films.

The N1s line in all samples and all angles was symmetrical and could thus be fitted by just one singlet of 2.2 eV half width. Its binding energy of 399.0 eV is consistent with the presence of C—N, C=N, and C≡N in organic polymers (amines, imines, and nitriles). Here, too, the rather broad singlet width is suggestive of a range of different but closely related structures.

Since the XPS spectra were rather featureless, they are not shown. The quantitative evaluations of the spectra are summarized in Table I. The most interesting observation from these analyses is the similarity between the elemental compositions of the PPy films on the anode and cathode, despite the considerable differences between their molecular structures, as was demonstrated by the FTIR analyses. These results are not at discrepancy with each other, however, as the differences that the RAIR analyses revealed, such as unsaturation, conjugation, and amines versus imines, are typically effects that cannot readily be identified by XPS.

The ^{1}H-NMR spectrum of the anode film dissolved in d_6-acetone is shown in Figure 2. Unlike the cathode film which did not dissolve, the anode film went into solution readily, suggesting a less crosslinked type of film. The overall appearance of the spectrum resembles that of an irregular polymer with protons in many different magnetic environments.[17] This makes a quantitative structural analysis of the film impossible, but a qualitative interpretation can be attempted based on the chemical shifts.

The intense peak at 1.19 ppm is characteristic of a long chain of hydrocarbons composed of methylene groups.[18] The spectrum also shows peaks which can be attributed to methylene groups on heteroatoms. This appears to be the case for the peak at 2.6 ppm, where a methyne- or methylene-group is adjacent to either an sp^3 or sp^2 nitrogen. Similarly, the peak at 3.5 to 3.6 ppm usually signifies an alkyl group attached to an oxygen, as found in an ether or ester. The broad peak at 2.96 ppm can be interpreted as a proton on an aliphatic amine.[17] The downfield proton peaks ranging from 6.43 to 7.48 ppm can be attributed to either conjugated olefins or olefins with adjacent heteroatoms. This reasoning is based on the fact that the peaks exhibit a larger downfield shift than expected for normal olefinic protons[17] and that no aromatic rings can be detected in the IR spectra. The broad peak at 8.5 ppm is representative of an amide proton, while the peak at 5.95 ppm could be caused by a proton directly attached to an sp^2 nitrogen or an amine-group attached to a conjugated system.

Table I XPS Data for PPy Films on Anode and Cathode

Take-off Angle	Peak	Binding Energy (eV)	State	Anode	Cathode
15°			C/N	7.0	7.8
	C1s	—	—	83.8%	83.8%
	C1s-1	284.6	C—C, C—H	72.9%	68.2%
	C1s-2	286.1	C—N, C=N	10.8%	13.2%
	C1s-3	287.6	$\rangle C=$	0.2%	1.9%
	N1s	399.0	N—C, N=C	12.2%	10.8%
	O1s	531.5	O=C$\langle$	4.0%	5.9%
75°			C/N	5.7	6.3
	C1s	—	—	82.2%	82.4%
	C1s-1	284.6	C—C, C—H	71.2%	67.1%
	C1s-2	286.1	C—N, C=N	10.8%	14.3%
	C1s-3	287.6	$\rangle C=O$	0%	1.0%
	N1s	399.1	N—C, N=C	14.5%	13.0%
	O1s	531.4	O=C$\langle$	3.4%	4.6%

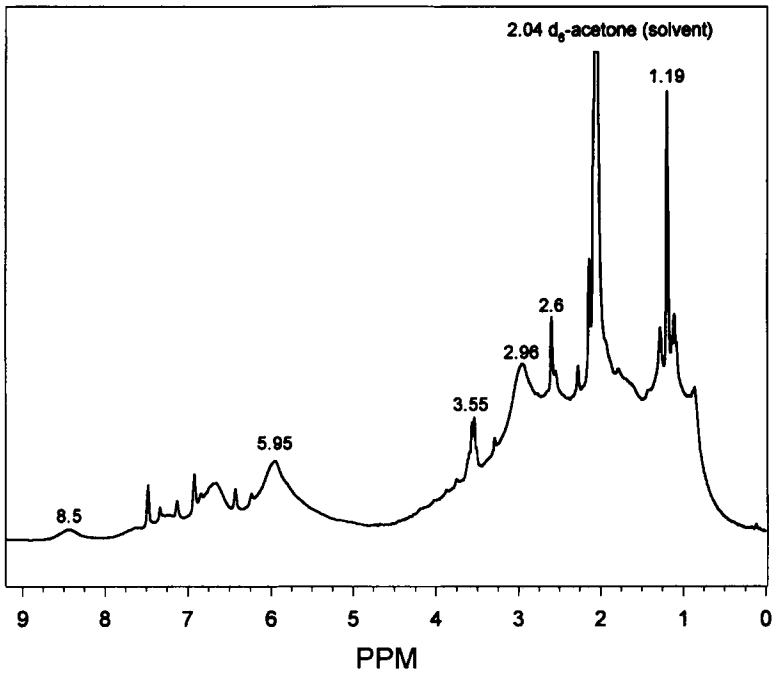

Figure 2 ^{1}H-NMR spectrum of a PPy film deposited on stainless steel as anode; dissolved in d_6-acetone; conditions as in Figure 1(a) for peak assignments see text.

Summarizing, the ^{1}H-NMR spectrum supports the interpretation of the coating on the anode as a film consisting mainly of long, noncrosslinked chains of saturated hydrocarbons and olefins with nitrogen present in the form of amines and imines.

The UV-VIS spectra of the PPy films are presented in Figure 3. Spectrum *A* shows the UV-VIS absorption of the film with electrical connection established to the anode. The spectrum of the film electrically connected to the cathode is represented by spectrum *C*. The complexity of the films prevents a quantitative interpretation, but general trends can be observed.

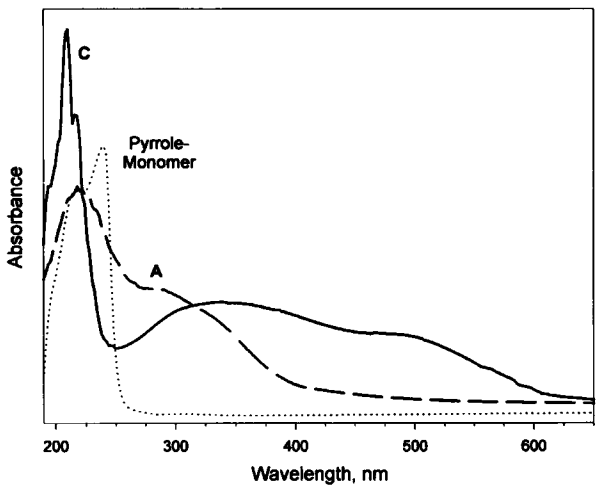

Figure 3 UV-VIS spectra of the pyrrole monomer and of PPy films deposited on gold-coated cuvettes; *A*: anode; *C*: cathode; conditions as in Figure 1(a).

In agreement with the IR and the NMR spectra, the UV-VIS spectra also demonstrate that the PPy films do not resemble the structure of the monomer or the one of the highly ordered electrochemically polymerized polypyrroles.[19] While the anode film does not exhibit any absorption over 400 nm, the film on the cathode displays a broad adsorption from 250 nm to 600 nm with several underlying bands, indicating a conjugated system with heteroatoms.[20] The fact that there is no absorption higher than 400 nm in the case of the anode implies that these films have almost no wide-range conjugation.

The cyclic voltammograms (CV) of the films deposited on platinum disk electrodes with a surface area of 0.03 cm^2 are shown in Figure 4(a–d). It was verified that the film structure on platinum resembles closely the one on stainless steel by coating a highly polished platinum sheet and obtaining RAIR spectra.

Three nominally identical electrodes were employed. Prior to deposition they were characterized by CV in 10 m*M* $K_3[Fe(CN)_6]$. The responses of the three electrodes were identical within a few per-

cent. One electrode was left untreated and used for comparison purposes in all subsequent electrochemical experiments. The response for the cathode film in 0.2*M* KCl at a sweep rate of 50 mV/sec is shown as *A* in Figure 4a. The signal remained essentially invariant under further cycling with no significant change seen even after 100 cycles. Repeating the experiment in a solution containing 10 m*M* $K_3[Fe(CN)_6]$ produced basically the same result. No effect of the electrochemically active anion could be seen. This is viewed as an indication that the film is essentially impermeable to the ions employed in aqueous solution and that it remains intact with no significant amount of exposed metal surface.

The electrode was then transferred into acetonitrile (ACN) containing 0.2*M* tetraethylammonium fluoroborate (TEBF) with the results for a 50 mV/sec scan shown as *B* in Figure 4(a). This response is significantly different from the aqueous results and more closely resembles an unmodified platinum electrode response under these conditions.

When this electrode is then returned to the aqueous 0.2*M* KCl-10 m*M* $K_3[Fe(CN)_6]$ solution, the ferricyanide couple is now clearly observable (shown as *A* in Fig. 4(b)) although far smaller in magnitude than for the untreated bare electrode. Further soaking of the coated electrode for 70 h and repeating the 0.2*M* KCl-10 m*M* $K_3[Fe(CN)_6]$ experiments produces the higher current values and more sigmoidal shape displayed as *B* in Figure 4(b).

The observed results suggest strongly that exposure of the cathode film to ACN results in structural changes in the film allowing easier access of solution molecules and solvated ions to the platinum electrode surface. In comparison to the very resistive and impenetrable cathode film, the first cyclic voltammogram of the anode film in aqueous 0.2*M* KCl exhibited a fairly high background current as shown in Figure 4(c). This suggests, in agreement with the spectroscopic data, a much less crosslinked type of film that permits diffusion of solution molecules and solvated ions. The first sweep in aqueous 10 m*M* $K_3[Fe(CN)_6]$ solution, at a scan rate of 10 mV/sec, is displayed in Figure 4(d). It shows a very distinct current response, also indicating that the ferricyanide ion can readily diffuse through the film and react at the platinum surface.

It is noticeable that the ferricyanide response in the case of the anode film and, to a certain extent, of the cathode film as well, resembles that of a purely diffusion-limited process usually seen in microelectrode studies.[21] The measured current on the other hand is two to three orders of magnitude higher than for a 10 μm disk microelectrode. This suggests that the film could have been partially lifted from the platinum surface resulting in a multitude of very small microblisters at the film-metal interface. Therefore, the film seems to act like an array of microelectrodes.[22] Further investigation into this interesting and potentially useful phenomenon are currently under way in our laboratory.

The cyclic voltammetric response of the coated platinum electrodes supports the spectroscopic interpretation of the cathode film, having largely a highly crosslinked character, while the anode film exhibits much less crosslinking.

Previously published[11] STM images of the cathode film are essentially featureless. In the anode case shown in Figure 5 it is clear that this surface is not the same type of dense, smooth coating. In concurrence with the results of the other techniques employed, the STM image of the anode film displays a high amount of irregularity with 30 nm diameter-depressions detectable.

DISCUSSION AND CONCLUSIONS

In this work, pyrrole films polymerized from a DC-plasma were simultaneously deposited on metallic substrates attached to the cathode and the anode. Neither film resembled electrochemically polymerized pyrrole, in agreement with previous studies by others in which pyrrole was polymerized in an RF plasma.[4] Apparently, the pyrrole ring structure is not maintained in a DC plasma either. It was found that the films formed on the cathode possessed the usual properties of plasma-polymerized organic materials reported in the literature.[8] The films appeared to be highly crosslinked and insoluble in organic solvents. Experimental evidence was presented that the cathode polymer exhibited a fair amount of conjugation. The films are impervious to inorganic ions and the surface was found to be reactive to oxygen. As seen by STM, the film exhibited no strong topographic feature.

By contrast, the films formed on the anode showed remarkably different properties. To our knowledge, the structure of films deposited on anodes in DC plasma reactors has not yet been compared in any detail to films formed simultaneously on the cathode. Since the DC reactor has not been extensively employed in recent plasma polymerization studies and because the deposition rate on the anode is at least an order of magnitude less than on the cathode,[10,11] anode films have been largely ig-

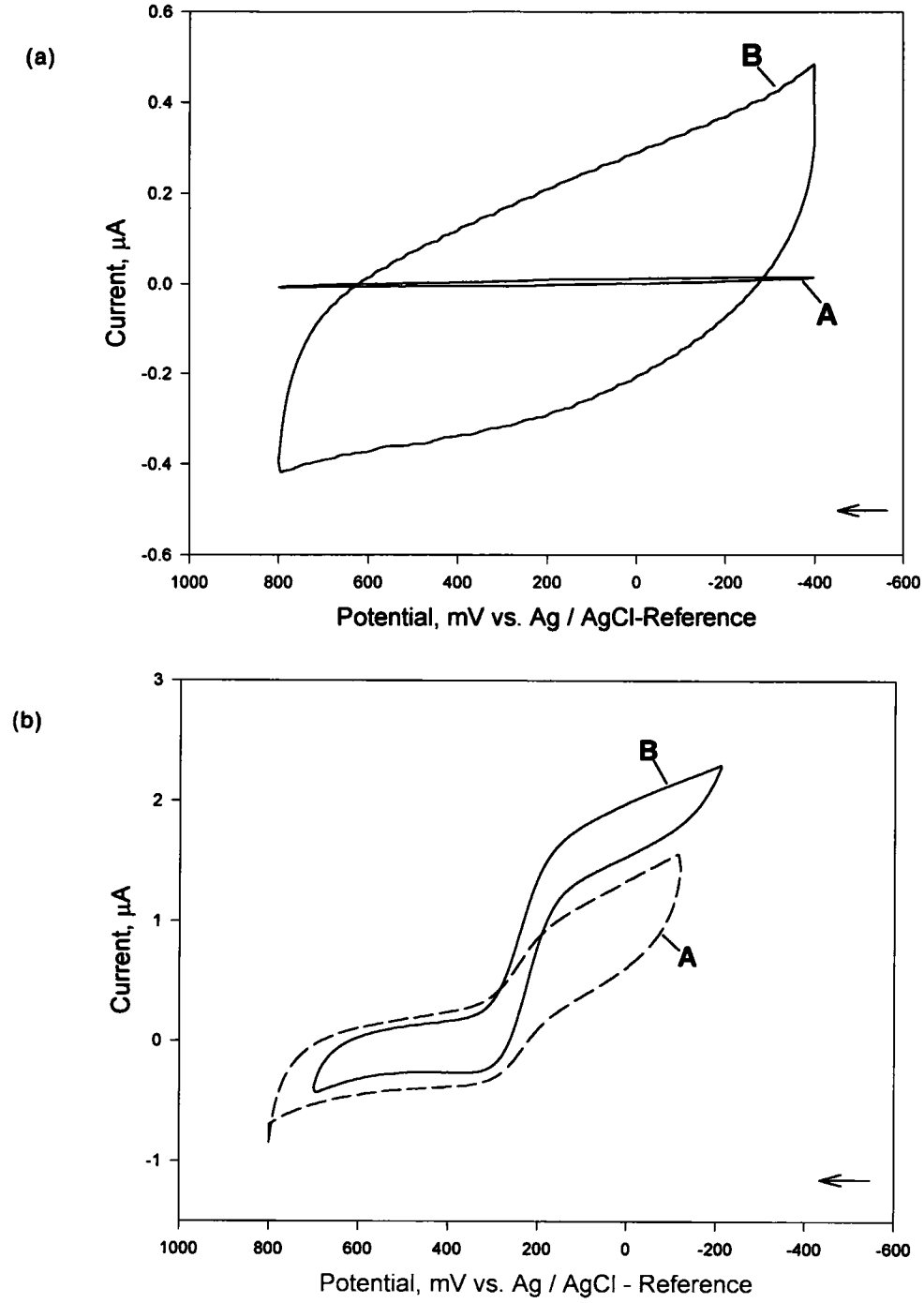

Figure 4 (a) Cyclic voltammograms of PPy film deposited on Pt-disk electrode as cathode; sweep rate 50 mV/sec; *A*: 100th scan in aqueous 0.2*M* KCl solution; *B*: 2nd scan in acetonitrile with 0.2*M* tetraethylammonium tetrafluoroborate. (b) Cyclic voltammograms of PPy film deposited on Pt-disk electrode as cathode; sweep rate 10 mV/sec; *A*: scan taken in aqueous 0.2*M* KCl/10 m*M* $K_3[Fe(CN)_6]$ solution; *B*: scan taken in aqueous 0.2*M* KCl/10 m*M* $K_3[Fe(CN)_6]$ after film was soaked in acetonitrile for 70 h. (c) Cyclic voltammograms of PPy film deposited on Pt-disk electrode as anode; sweep rate 50 mV/sec; first scan in aqueous 0.2*M* KCl solution. (d) Cyclic voltammograms of PPy film deposited on Pt-disk electrode as anode; sweep rate 10 mV/sec; first scan in aqueous 0.2*M* KCl/10 m*M* $K_3[Fe(CN)_6]$.

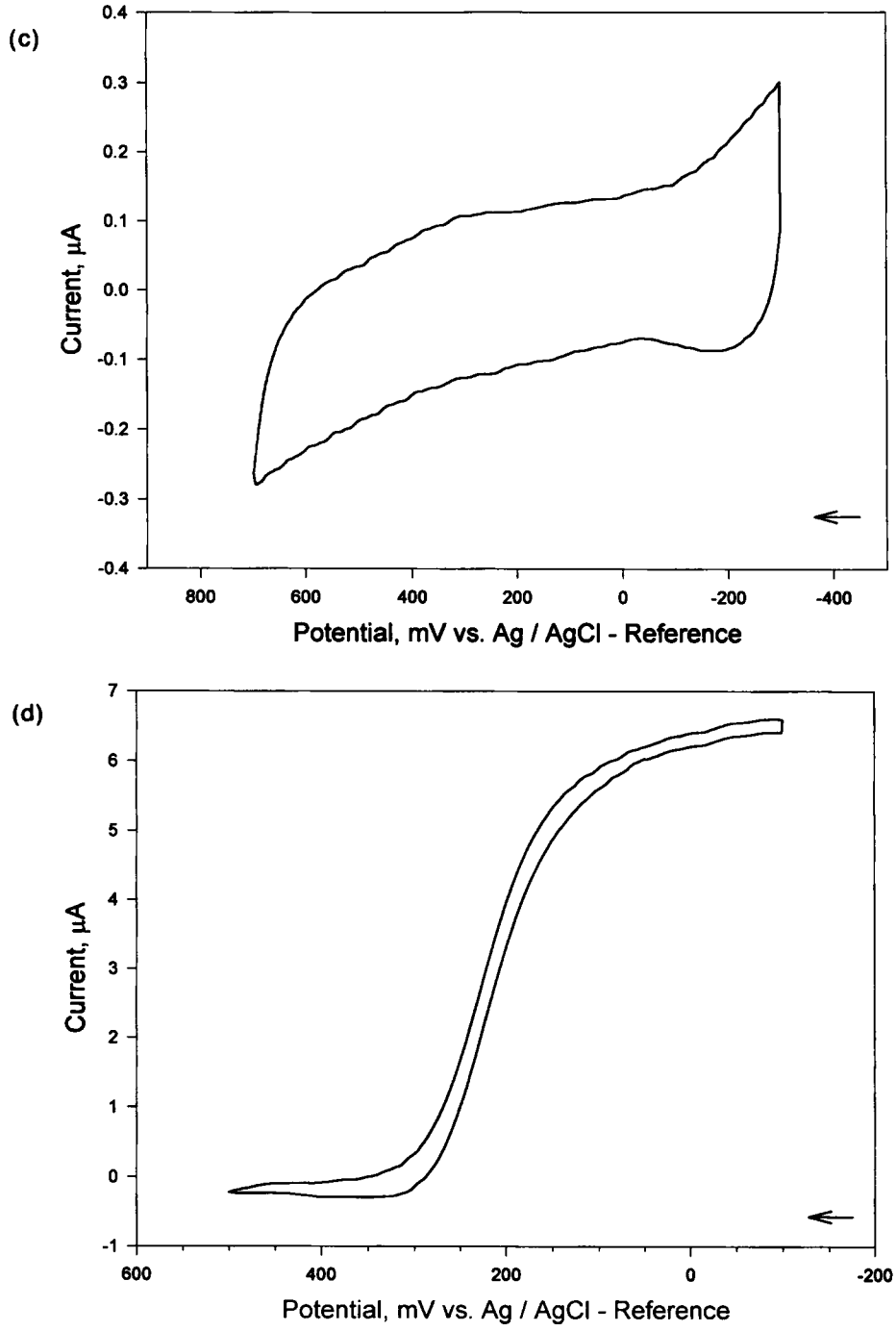

Figure 4 (*Continued from the previous page*)

nored. However, a comparison of the structures of the films formed on both electrodes might reveal some valuable insight into the mechanisms of film growth and the relative effects of radicals, positive or negative ions and electrons on the film growth and structure.

The anode films were found to be less crosslinked and less conjugated and were readily soluble in organic solvents. Further, they seemed to contain longer hydrocarbon chains than the cathode film. The overall elemental composition was, however, very similar for both films. The anode film had a

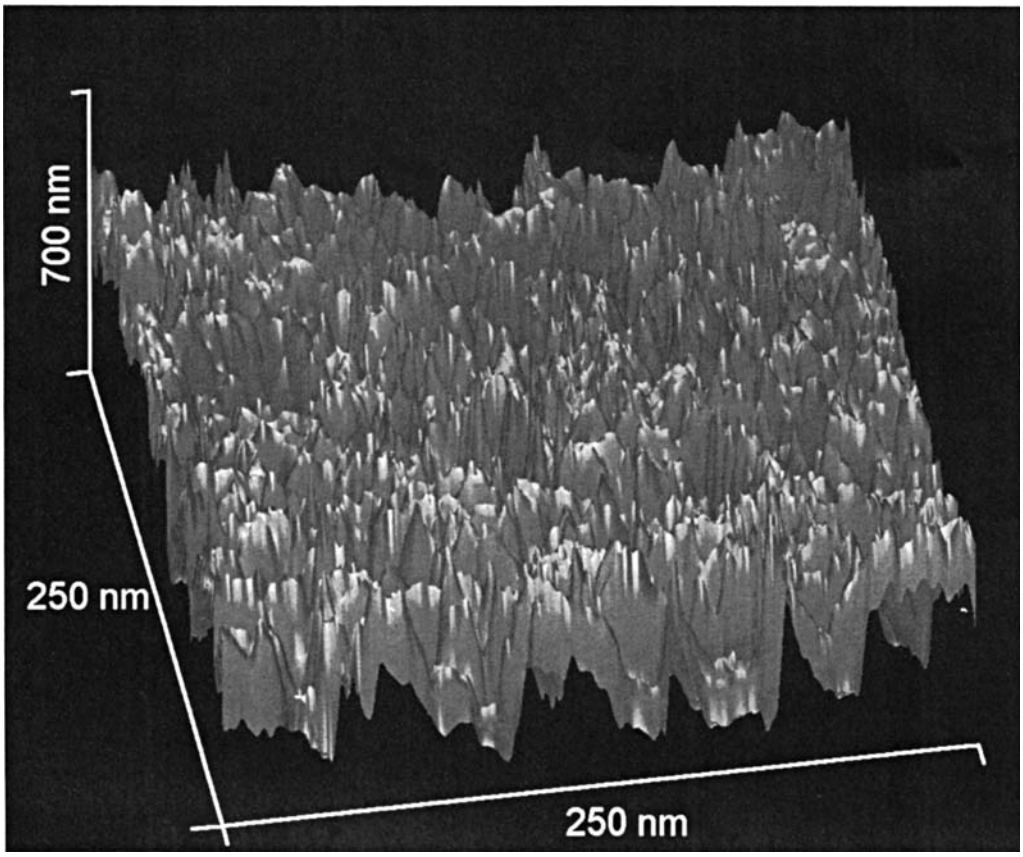

Figure 5 STM image of PPy film deposited on stainless steel as anode, bias voltage: −50 mV, tunneling current: −2 nA.

slightly lower surface reactivity for oxygen. It showed strong topographic features. Due to the lower crosslink density, the anode films readily permit the diffusion of water and solvated ions to the metal-film interface. Even cathode films of the same thickness as the anode films studied here, were considerably less penetrable than the anode film.

The observed structural differences and compositional similarities between the two types of films suggest the following model for the polymerization of pyrrole in a parallel-plate DC reactor. Since the elemental compositions (as per XPS analysis) of the anodic and cathodic films are virtually identical, it is reasonable to assume that the film grows largely by the same mechanism on both electrodes. Such a mechanism is most likely a free radical mechanism, as ionic mechanisms should be different for positively and negatively charged electrodes. The C/N ratio in both deposits is 7 : 1 as opposed to 4 : 1 in the monomer, suggesting that, although part of the nitrogen is lost, both *N*-containing and *N*-free radicals occur in the plasma and contribute to the film growth by radical polymerization.

The similarity in elemental compositions on both sides further indicates that sputtering by the impinging ions is not a major factor. This is a reasonable assumption since it has been well documented that H^+ is the dominant positive species in plasmas of hydrocarbons.[6,8,23] Protons have a very low efficiency for selectively sputtering heavier atoms such as N, O or C. Thus, the H^+ bombardment does not significantly alter the elemental composition of the growing deposit. However, the effects of H^+ impingement are removal of hydrogen from the polymer, resulting in crosslinked, conjugated and dense structures,[24] and in the formation of radical sites at the film surface. Such sites react with activated species in the plasma. Thus, a higher ion current in hydrocarbon plasmas generally leads to an increased film growth.[23] The higher deposition rate at the cathode is thus simply linked to the higher plasma intensity (negative glow) in front of the cathode as

compared to the much weaker intensity in the anode region (positive column). The secondary electrons that are emitted from the (metallic) cathode sustain the high intensity in the negative glow region of the plasma.

As a result of the sputtering of H-atoms from the growing cathodic films, it can be expected that the deposits will increase their content of carbon-carbon and carbon-nitrogen double bonds. One could speculate that this ion bombardment abrades any topographic features. These effects are seen in the RAIR and UV-VIS spectra and in the STM images.

The films growing on the anode will, in principle, be bombarded by negative ions and by electrons. Impingement of the latter will not lead to conjugational or sputtering effects, but will only result in activation, i.e., formation of radical sites. Thus, they are mainly responsible for film growth on the anode. Long-lived negative ions cannot be expected in high concentrations from the monomer pyrrole. Some CN^- ions will undoubtedly be present, but their concentration is expected to be much lower than that of H^+.

We thus postulate that the growth mechanism of the plasma polymer from pyrrole is on both electrodes by radical polymerization initiated by radical sites in the film surface. These radical sites are created by H^+ impinging on the cathode and by electrons on the anode. This mechanism by itself does not necessarily result in highly crosslinked polymers. However, on the cathode there is a constant bombardment of the growing films by protons which results in several effects, viz. a) removal of hydrogen atoms from the polymeric structure, b) dissolution of hydrogen in the films, c) crosslinking of the films, and d) trapping of radical sites in the film structure; this latter effect results in a film with a high affinity for oxygen when exposed to the atmosphere.

An important conclusion of this work is that in a simple parallel-plate DC reactor the positive ion bombardment of the plasma polymer does not seem to alter the film composition, but it has a considerable effect on the film structure, such as crosslinking and degree of conjugation.

In summary, it can be stated that a DC reactor for direct plasma polymerization of organic monomers (i.e., in the absence of carrier gases) is a simple but versatile tool in terms of mechanism of polymerization. The structure of the polymeric deposit can be manipulated in a variety of ways. For instance, the potential of the substrate (determined by the dissipated power) has an effect on the film structure by regulating the energy of the ions that impact the growing film. The pressure also has an effect since it controls the intensity of the bombarding ion flux. As we have recently demonstrated, films of pyrrole deposited at high pressure contain more dissolved hydrogen than when deposited at lower pressure.[11] This observation supports our view of H^+ as the dominant type of ions carrying the total ion current.

In this paper we have demonstrated that another method for manipulating the structure of the deposits obtained from pyrrole in a simple DC design is by depositing on the anode rather than on the cathode. The films obtained there are true polymers, i.e., they are adherent solids and are not powdery or oily, but they are considerably more linear in structure and hence softer and more soluble in solvents than the polymers deposited on the cathode. Such properties suggest possible applications as coatings in situations where brittle films, typical of cathodic deposits, are undesirable, e.g., on flexible substrates.

The authors thank Mr. Herman Holt for acquisition of the NMR spectra and Dr. Rohit Pobat for assisting in the XPS measurements.

REFERENCES

1. G. P. Gardini, *Adv. Heterocyclic Chem.*, **15,** 67 (1973).
2. A. F. Diaz and K. K. Kanazawa, *Chem. Scr.*, **17,** 145 (1981).
3. T. A. Skotheim, ed., *Handbook of Conducting Polymers,* Marcel Dekker, New York, 1986.
4. T. Kojima, H. Takaku, and Y. Urata, *J. Appl. Polym. Sci.*, **48,** 1395 (1993).
5. M. Tazaki, H. Aizawa, and T. Homma, *Chem. Lett.*, 1905 (1994).
6. O. Aucello and D. L. Flamm, eds., *Plasma Diagnostics: Volume I, Discharge Parameters and Chemistry; Volume 2, Surface Analysis and Interactions,* Academic Press, San Diego, 1989.
7. W. J. van Ooij, D. Surman, and H. K. Yasuda, *Prog. Org. Coat.*, **25,** 319 (1995).
8. H. K. Yasuda, *Plasma Polymerization,* Academic Press, Orlando, 1985.
9. W. J. van Ooij, P. J. Barto, S. Eufinger, K. D. Conners, and N. Tang, *Proc. Symp. Pol. Surf. Interfaces, SPE ANTEC,* Boston, MA, May 8–11, 1995; in press.
10. W. J. van Ooij, S. Eufinger, and S. Guo, submitted to *Plasma Chem. Plasma Proc.*
11. W. J. van Ooij, S. Eufinger, and T. H. Ridgway, *Plasmas and Polym.*, in press.
12. S. Eufinger, W. J. van Ooij, and T. H. Ridgway, *Surf. Interface Anal.*, in press.

13. W. J. van Ooij, N. Tang, K. D. Conners, and P. J. Barto, *Proc. Intern. Adhesion Symp. IAS 94 Japan,* Yokohama, November 6–10, 1994; in press.
14. G. B. Street, T. C. Clarke, M. Krounbi, K. K. Kanazawa, V. Lee, P. P. Fluger, J. C. Scott, and G. Weiser, *Mol. Cryst. Liq. Cryst.,* **83,** 253 (1982).
15. G. Socrates, *Infrared Characteristic Group Frequencies,* Wiley, New York, 1994 and references therein.
16. C. J. Pouchert, *The Aldrich Library of Infrared Spectra,* Edition III, Aldrich Chemical Company, 1981, p. 1565.
17. N. F. Chamberlain, *The Practice of NMR Spectroscopy,* Plenum Press, New York (1974).
18. Q-T. Pham, R. Petiaud, and H. Waton, *Proton and Carbon NMR of Polymers,* Vol. 2, Wiley, New York (1983).
19. K. Yakushi, L. J. Lauchlan, T. C. Clarke, and G. B. Street, *J. Chem. Phys.,* **79,** 4774 (1983).
20. R. M. Silverstein, G. C. Bassler, and T. C. Morrill, *Spectrometric Identification of Organic Compounds,* Wiley, New York (1991) and references therein.
21. R. M. Wightman and D. O. Wipf, *Voltammetry at Ultramicroelectrodes,* in *Electroanalytical Chemistry,* A. J. Bard, Ed., Marcel Dekker, New York (1985).
22. Zhang, C. Wang, and X. Zhou, *Anal. Chim. Acta,* **265,** 27 (1992).
23. H. Biederman and Y. Osada, *Plasma Polymerization Processes,* Elsevier, Amsterdam, 1992.
24. W. J. van Ooij and R. S. Michael, in *Metallization of Polymers,* ACS Symposium Series No. 440; ACS, Washington, DC, 1990, p. 60.

Received November 17, 1995
Accepted March 1, 1996